Journal of Neonatal Surgery
ISSN(Online): 2226-0439
Vol. 14, Issue 4 (2025)
https://www.jneonatalsurg.com

OPEN ACCESS

Ultrasonic Leak Detection Using MEMS Sensors For Industrial Pneumatic Pipeline Monitoring

Bijoy Laxmi Koley[1*], Anupam Kumar Biswas[2], Moloy Mukherjee[3], Surajit Batabyal[4], Subhadra Deb Roy[5], Subhasish Debroy[6], Saradindu Mondal[7]

[*1]Department of Electrical Engineering, Dr. B. C. Roy Engineering College, Durgapur, West Bengal.
Email ID: bijoylaxmi.koley@bcrec.ac.in

[2]Department of Civil Engineering, Dr. B. C. Roy Engineering College, Durgapur, West Bengal.
Email ID: anupam.biswas@bcrec.ac.in

[3]Department of Electronics & Communication Engineering, Dr. B.C. Roy Engineering College, Durgapur, West Bengal.
Email ID: moloy.mukherjee@bcrec.ac.in

[4]Department of Electronics & Communication Engineering, Dr. B.C. Roy Engineering College, Durgapur, West Bengal.
Email ID: surajit.batabyal@bcrec.ac.in

[5]Department of Electronics & Communication Engineering, Dr. B.C. Roy Engineering College, Durgapur, West Bengal.
Email ID: subhadra.debroy@bcrec.ac.in

[6]Bachelor of Computer Application, Dr. B.C. Roy Academy of Professional Courses, Durgapur, West Bengal.
Email ID: subhasish.debroy@bcrec.ac.in

[7]Department of Electrical Engineering, Dr. B.C. Roy Engineering College, Durgapur, West Bengal.
Email ID: saradindu.mondal@bcrec.ac.in

Cite this paper as: Bijoy Laxmi Koley, Anupam Kumar Biswas, Moloy Mukherjee, Surajit Batabyal, Subhadra Deb Roy, Subhasish Debroy, Saradindu Mandal, (2025) Ultrasonic Leak Detection Using MEMS Sensors For Industrial Pneumatic Pipeline Monitoring. *Journal of Neonatal Surgery*, 14 (4), 632-644.

ABSTRACT

This study presents an ultrasonic leak detection system for industrial pneumatic pipelines utilizing MEMS-based sensors. The system incorporates a conical horn (electronic gun) design to enhance signal focusing and improve detection sensitivity. Controlled experiments were conducted using six leak diameters (1–6 mm) and six pressure levels (5–30 PSI). Fast Fourier Transform (FFT) analysis was employed for feature extraction, improving the system's robustness over conventional CWT-based methods. The CNN model achieved 90% accuracy for binary leak detection, while a reduced feature-based model maintained 88.9% accuracy with improved computational efficiency. Results indicate higher detection accuracy for larger leaks at elevated pressures, while small leaks at low pressures posed greater challenges. The integration of the conical horn significantly enhanced signal clarity, particularly in detecting minor leaks. The proposed system's effective balance of accuracy, sensitivity, and computational efficiency makes it suitable for real-time industrial monitoring applications.

Keywords: *Ultrasonic Leak Detection Using MEMS Sensors for Industrial Pneumatic Pipeline Monitoring*

1. INTRODUCTION

Leak detection in industrial pneumatic pipelines is crucial to prevent energy losses, equipment failures, and operational downtime. Studies indicate that undetected leaks in compressed air systems can account for 20–30% of total energy losses in industrial plants, resulting in significant financial and productivity impacts. Additionally, pipeline leaks may cause pressure drops that reduce the efficiency of pneumatic tools and machinery, further contributing to operational inefficiencies.

Various techniques have been explored for leak detection, including acoustic emission analysis, infrared thermography, and gas-sniffing sensors. Ultrasonic detection has emerged as a preferred method due to its ability to identify leaks from a distance and under noisy industrial conditions. However, traditional ultrasonic methods face limitations in detecting low-pressure leaks and small-diameter openings.

In this study, MEMS-based ultrasonic sensors are employed to improve detection sensitivity and provide real-time monitoring capabilities. To further enhance detection efficiency, a conical horn (electronic gun) design was introduced to

focus ultrasonic waves, improving signal strength and clarity. Combined with FFT-based feature extraction and a lightweight CNN model, this system effectively identifies leak-induced ultrasonic patterns while maintaining computational efficiency. The proposed solution demonstrates superior performance in distinguishing leak signals from background noise, especially for challenging low-pressure scenarios.

Several research groups have addressed pipeline defect detection using ultrasonic and acoustic emission (AE) methods, with evolving techniques over the past decades. Early work by Pollock and Hsu [1] pioneered the use of AE for leak detection, while Tani et.al. [2–4] introduced chaos theory for high-pressure gas leak detection in refining plants. Cruz et al. [5] and Li et al. [6] further advanced the field by combining AE techniques with machine learning for leak localization. Xu et al. [7] and Santos et al. [8] demonstrated that integrating mode decomposition with neural networks can improve both sensitivity and quantitative estimation of leak magnitude. Jian Li et al. [9] and Wang and Yao [10] showed that MEMS-based microphone arrays and aeroacoustic measurements are effective for capturing subtle leak signals.

In parallel, ultrasonic methods for surface crack detection in pipelines have also been explored. Yang et al. [11] employed Rayleigh wave analysis detect microcracks with high resolution. Zang et. al. [12] employed deep learning algorithm for microcrack detection. More recently, Cheng et al. [13] and Ahmed et al. [14] integrated Fast Fourier Transform (FFT) with convolutional neural networks (CNNs) to achieve leak detection accuracies above 80%. Lupea and Lupea [15] demonstrated similar success in gearbox fault detection using FFT and CNNs, emphasizing time–frequency representations. The authors in [16] proposed a self-coupled ultrasonic system that overcomes the limitations of coupling agents. Fan et al. [17] used encoder-decoder architecture for automatic crack detection on road pavements. Zhou et al. [18], Khan et al. [19], and Hamishebahar et al. [20] have contributed recent innovations by integrating 3D-printed sensor modules, advanced analog front-ends, and deep learning for portable, high-precision pipeline inspection. Collectively, these studies underscore a shift from conventional AE and chaos analysis to integrated FFT–CNN methodologies that significantly enhance detection reliability and resolution.

Early studies used acoustic emission and chaos theory for leak detection, while later works integrated MEMS sensors, mode decomposition, and machine learning for improved sensitivity and localization. Recent advances employ continuous wavelet transforms and CNNs, combined with sensor designs and 3D-printed modules, yielding high accuracy and portable pipeline monitoring systems.

This work presents a portable crack detection system that integrates a MEMS-based ultrasonic sensor, custom analog front-end, high-rate ADC, FFT signal processing, and CNN classification for real-time pipeline defect identification.

Proposed system integrates FFT and CNN on portable hardware, unlike conventional methods based solely on guided wave or visual inspections.

Main Contributions:

- Development of a lightweight, handheld system combining MEMS ultrasonic sensing with a dedicated analog front-end and high-rate digital acquisition.
- Novel fusion of FFT and CNN classification for accurate, real-time crack detection, replacing traditional continuous wavelet transform-based methods.
- Integration of a conical horn guide to enhance directional sensitivity, improving inspection accuracy over conventional designs.

The remainder of this paper is structured as follows: Section II presents the detailed design of the developed sensor system, including the ultrasonic sensor modules integrated with a conical horn guide, the analog front-end circuit, the analog-to-digital converter, and the overall system integration. The section also describes the digital signal processing framework implemented using a microcontroller and the application of the Fast Fourier Transform (FFT) for feature extraction. Section III outlines the experimental setup and data collection process, ensuring comprehensive evaluation of the proposed system. Section IV details the CNN-based classification framework, including database preparation, training, and validation processes. The Results are discussed in Section V, followed by an in-depth Discussion in Section VI that highlights the system's performance, limitations, and practical implications. Finally, Section VII concludes the paper by summarizing key findings and potential future enhancements.

2. SENSOR SYSTEM DESIGN

This section presents the comprehensive design of the proposed MEMS-based ultrasonic leak detection system, which integrates a conical horn guide, analog front-end circuitry, a high-rate analog-to-digital converter (ADC), and overall system integration. Each component is designed to maximize detection sensitivity, signal clarity, and real-time performance.

A. Ultrasonic Sensor Module The ultrasonic sensor module employs a MEMS-based ultrasonic transducer designed for high-frequency acoustic signal detection. MEMS sensors were selected for their compact size, low power consumption, and enhanced sensitivity to high-frequency leak-induced signals.

1) Conical Horn Guide Design To improve the system's detection range and directional sensitivity, a conical horn guide is integrated with the sensor module. The conical horn design follows acoustic wave focusing principles, enhancing signal strength by concentrating the incoming sound waves onto the MEMS sensor diaphragm. The conical profile was optimized to balance directional gain and operational bandwidth, ensuring improved signal focus without excessive attenuation of higher frequencies.

B. Analog Front-End Circuit

The analog front-end circuit is designed to condition the weak ultrasonic signals captured by the MEMS sensor, ensuring optimal signal integrity for subsequent processing. It begins with a pre-amplifier stage that employs a low-noise amplifier (LNA) to amplify the sensor output while minimizing noise contamination. The LNA provides adequate gain to enhance the low-amplitude ultrasonic pulses without introducing distortion. Following this, a band-pass filter is implemented to isolate the ultrasonic frequency band of interest, specifically between 10 kHz and 80 kHz. This filtering step effectively suppresses ambient noise and enhances signal clarity by focusing only on relevant frequency components. To maintain consistent signal strength under varying environmental conditions, an automatic gain control (AGC) circuit dynamically adjusts the gain based on the detected signal amplitude. This adaptive adjustment ensures stable signal levels, improving the robustness and reliability of the leak detection system in practical scenarios.

C. Analog-to-Digital Conversion A high-rate ADC (500 kS/s) digitizes the conditioned ultrasonic signals for subsequent digital processing. The ADC resolution was chosen to ensure accurate representation of the signal's amplitude and frequency content. Sampling at 500 kS/s effectively captures the ultrasonic signal's rich spectral characteristics, which are crucial for FFT-based feature extraction.

D. Microcontroller based Digital Signal Processing Framework The digitized signal undergoes FFT-based spectral analysis for extracting key frequency-domain features. The FFT implementation efficiently computes power spectra, peak frequency, bandwidth, and spectral energy. These features provide critical information for distinguishing leak-induced signals from normal background noise. The digital processing framework is implemented on a microcontroller, ensuring efficient real-time data handling and analysis.

E. System Integration All hardware modules are integrated into a lightweight, handheld device for on-site inspections. The sensor module, conical horn guide, analog front-end, and ADC are housed in a robust 3D-printed casing designed to withstand industrial environments. The system is powered by a rechargeable battery pack, ensuring portability and extended field operation. The functional block diagram of the integrated system is shown in Figure 1.

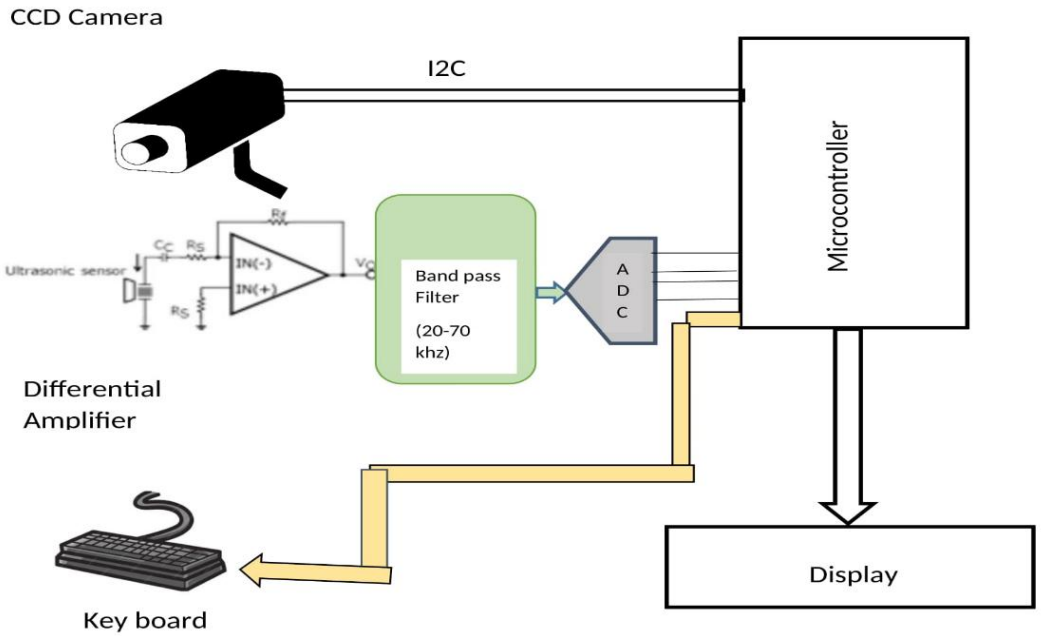

Figure 1. Block diagram of the proposed ultrasonic leak detection system, illustrating the sensor module, analog front-end, ADC, microcontroller, and signal processing stages for pipeline crack detection.

3. EXPERIMENTATION AND DATA COLLECTION

A. Experimental Setup

The experimental setup, illustrated in **Figure 2**, was designed to emulate industrial pneumatic pipeline conditions for leak detection performance assessment. The setup comprises the following key components:

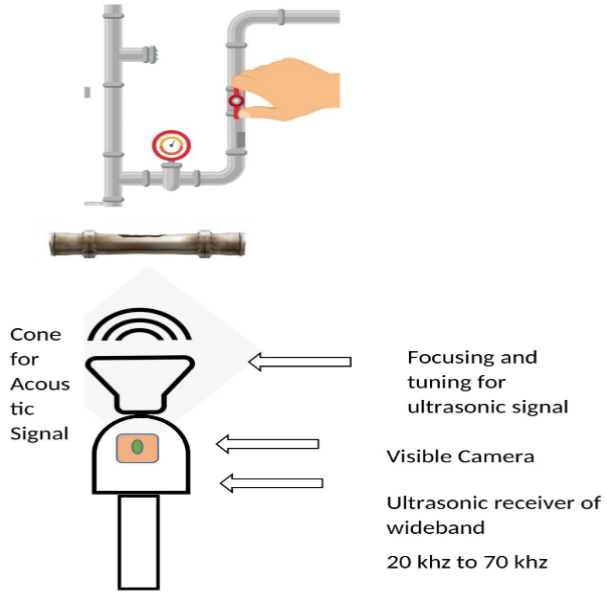

Figure. 2. Experimental setup for evaluation of the performance of the ultrasonic leak detection unit.

The experimental setup consisted of a MEMS-based ultrasonic sensor (20 kHz to 70 kHz) integrated with an analog front-end circuit, ADC, microcontroller unit, and data processing system. The sensor was mounted within a 3D-printed electronic gun structure to provide precise positioning and improve directional control. A conical horn guide (100 mm length, 9.5° field-of-view) was employed to enhance directional sensitivity and minimize noise interference.

B. Experimental Conditions

To assess the system's performance across practical conditions, the experiments included:

- Six Leak Sizes: Controlled leaks were created in the pipeline with diameters ranging from 1 mm to 6 mm.
- Six Pressure Levels: To emulate varying industrial conditions, pressures of 5, 10, 15, 20, 25, and 30 PSI were applied.

To ensure data reliability and variability, three sets of data were collected for each combination of leak size and pressure level. Similarly, for the no-leak condition, data was collected at all six pressure levels with three repetitions for each condition. This comprehensive data collection resulted in 236 datasets as follows:

(6 leak sizes×6 pressure levels×3 repetitions)+(6 no leak conditions× 6 pressure levels× 3 repetitions) =236 datasets

Additionally, 106 sets of no-leak data were collected, consisting of background noise to improve model accuracy in distinguishing normal conditions from leak-induced signals.

C. Recorded Signal Analysis

The recorded ultrasonic signals exhibited distinct characteristics influenced by both leak size and pressure levels. Larger leaks consistently produced higher signal amplitudes, while smaller leaks generated comparatively weaker pulses. In terms of frequency behavior, smaller leaks were characterized by higher-frequency oscillations, whereas larger leaks displayed dominant lower-frequency components. Signal attenuation patterns revealed that smaller leaks experienced more pronounced signal decay, indicating weaker energy retention over time. Additionally, signals from smaller leaks exhibited greater irregularities, reflecting a lower signal-to-noise ratio, which posed challenges for accurate detection. The impact of pressure levels was also evident, as increasing pressure significantly enhanced the strength of ultrasonic emissions. This improvement in signal clarity under higher pressures played a crucial role in enhancing the system's ability to reliably detect leaks across varying conditions.

D. Data Collection and Database Formation

The collected data was systematically organized into a structured database to support the training and evaluation of the proposed model. Each dataset comprised multiple components to ensure comprehensive feature representation. The raw ultrasonic signals were recorded as time-domain data sampled at 500 kHz, providing a high-resolution capture of the acoustic waveforms. To facilitate frequency analysis, the Fast Fourier Transform (FFT) was applied, generating frequency-domain representations essential for effective feature extraction. Additionally, distinct feature vectors were extracted to enhance the model's ability to identify key signal characteristics. These features included peak frequency, which highlights the dominant frequency component; bandwidth, which reflects the spread of the signal's frequency content; spectral energy, representing the cumulative energy content; and Shannon entropy, which quantifies the signal's complexity and randomness. Each dataset entry was carefully labeled based on its corresponding leak size, pressure condition, or no-leak status, ensuring robust training and enabling the model to accurately distinguish between different experimental conditions.

The collected database was divided into training (70% of the data) and testing (30% of the data) sets to ensure balanced representation of all experimental conditions.

4. CNN-BASED CLASSIFICATION

A. Database

The collected ultrasonic data was organized into a structured database, where each sample was labeled according to its corresponding leak size or classified as background noise (no-leak condition). Frequency spectra were generated using the Fast Fourier Transform (FFT), effectively converting time-domain signals into frequency-domain representations. These FFT scalograms served as input features for the CNN model, enabling precise classification of defect dimensions. The database was structured to ensure balanced representation across various leak sizes and pressure conditions.

B. Proposed Lightweight CNN Architecture

To enable efficient real-time classification on a resource-constrained microcontroller, a lightweight convolutional neural network (CNN) architecture was designed. The proposed model leverages depthwise separable convolution layers to reduce computational complexity while retaining high classification performance. The architecture is depicted in Figure 3.

Architecture Overview:

- Input Layer: Accepts FFT scalogram images as input, representing the frequency-domain data.
- Depthwise Separable Convolution Layers: Each convolution step is split into two operations:
    - Depthwise Convolution: Performs channel-wise filtering to capture spatial information.
    - Pointwise Convolution: Combines features from all channels to enhance feature integration.

The depthwise separable convolution reduces computational load without compromising detection accuracy. Mathematically, this is expressed as:

$$Y_{output} = \sum_{c=1}^{C} (X_{input} * K_{depthwise}) * K_{pointwise}$$

Where $\boldsymbol{X}_{input}$ is the input feature map, $K_{depthwise}$ is the depthwise convolution filter, and $K_{pointwise}$ is the pointwise filter.

- **PReLU Activation Function:** A parametric ReLU activation function is employed to introduce non-linearity and improve convergence. It is defined as:

$$f(x) = \begin{cases} x & \text{if } x > 0 \\ \alpha x & \text{if } x \leq 0 \end{cases}$$

Where α is a learnable parameter that adapts to the data.

- **Global Average Pooling (GAP):** Reduces the spatial dimensions of feature maps to a single vector by computing the average of each feature channel. GAP effectively minimizes overfitting while preserving key information.
- **Fully Connected Layer:** Generates the final classification output, mapping extracted features to their respective class labels.

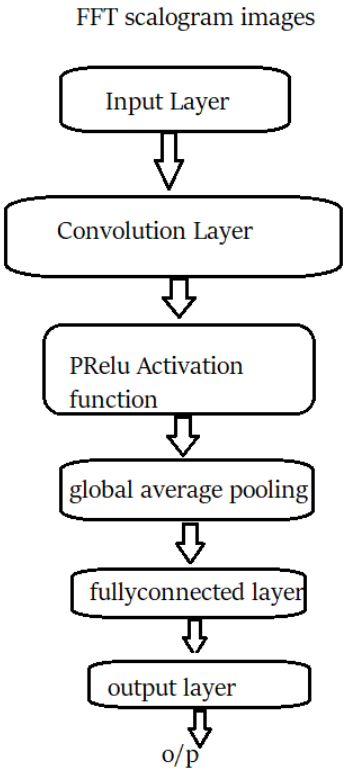

C. Testing and Validation

The CNN model was trained using the labeled dataset comprising ultrasonic leak signals and no-leak background noise. The training process incorporated:

- **Batch Normalization:** To stabilize learning and accelerate convergence.
- **Adaptive Learning Rate:** Employed to dynamically adjust the learning rate for optimal convergence.
- **Adam Optimizer:** Selected for its efficient gradient-based optimization in noisy environments.

The trained model was validated using unseen data samples, where performance was assessed based on **accuracy**, **precision**, and **recall**. Results demonstrated that the lightweight CNN effectively classified various leak sizes while ensuring low latency, meeting the requirements for real-time detection.

D. Feature Analysis

To enhance classification accuracy and ensure robust detection across diverse conditions, key features were extracted from the ultrasonic signals:

- **Energy per Scale:** Provides insight into the energy distribution across distinct frequency bands.
- **Total Energy:** Represents the cumulative energy content of the signal.
- **Energy in High-Frequency Band (>30 kHz):** Focuses on critical high-frequency components, improving sensitivity to smaller leaks.
- **Shannon Entropy:** Measures the complexity and randomness of the signal, aiding in distinguishing leak signals from noise. It is defined as:

$$H(X) = -\sum_{i=1}^{N} p(x_i) \log_2 p(x_i)$$

Where $p(x_i)$ denotes the probability distribution of the signal's amplitude values.

These extracted features collectively enhance the CNN model's ability to differentiate between various leak sizes, pressure conditions, and background noise, ensuring improved detection accuracy and system robustness.

5. RESULTS AND DISCUSSION

This section presents the results obtained from the experimental study and the performance evaluation of the proposed ultrasonic leak detection system. The findings are discussed in detail by analyzing the recorded signal characteristics, frequency spectrum trends, feature behavior, and model performance. Each aspect is supported by relevant figures to highlight key observations and insights.

A. Recorded Signal Analysis

Figure 3 presents the ultrasonic signal waveforms recorded from six different leak diameters (ranging from **1 mm to 6 mm**) over a **100 ms period** at a constant pressure of **20 PSI**. The recorded signals exhibit clear distinctions in both amplitude and frequency characteristics. As the leak diameter increases, the amplitude of the waveform progressively rises, indicating stronger acoustic emissions for larger leaks. Smaller leak signals tend to have higher-frequency content, while larger leaks exhibit more dominant low-frequency components. This behavior is attributed to the increased turbulence and airflow intensity associated with larger leaks.

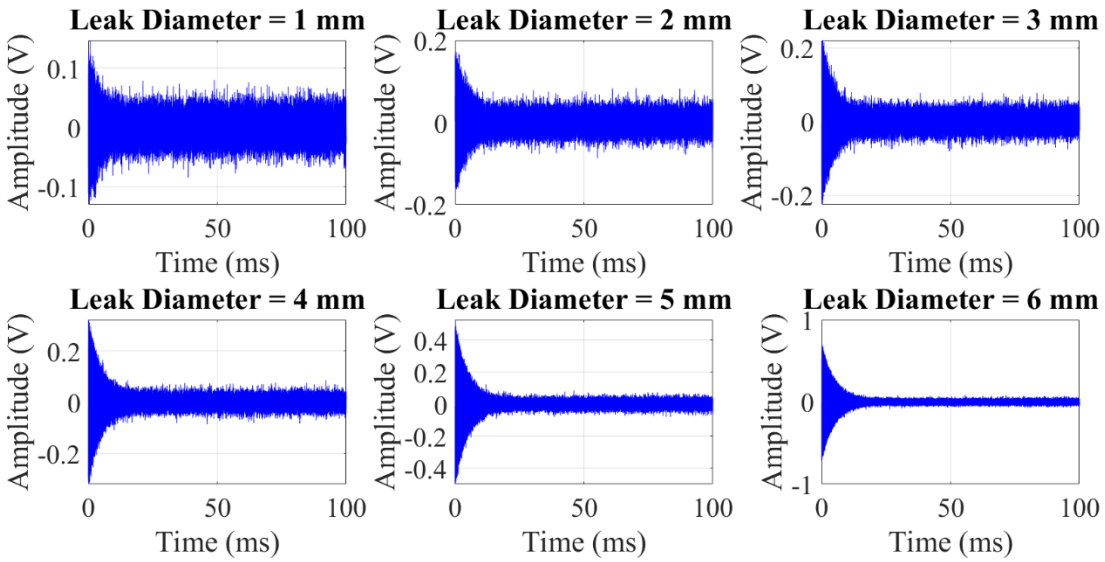

Figure 3: Ultrasonic signal waveforms corresponding to six different leak diameters (1 mm to 6 mm) recorded over a 100 ms period, at 20 PSI pressure. Each waveform demonstrates variations in amplitude and frequency characteristics.

Additionally, smaller leak signals show more pronounced noise fluctuations and irregular patterns, reflecting their weaker acoustic emissions and lower signal-to-noise ratios. Conversely, the waveforms for larger leaks display more stable and defined pulses, making them easier to identify using waveform analysis techniques. The increasing amplitude trend with larger leak diameters demonstrates the system's ability to effectively capture varying signal intensities corresponding to different leak sizes.

Figure 4 illustrates the recorded ultrasonic signals for a **2 mm diameter leak** subjected to six different pressure levels, ranging from **5 PSI to 30 PSI**. The results reveal a clear correlation between pressure intensity and signal amplitude. At **5 PSI**, the signal exhibits a weak initial pulse, indicating limited acoustic emission under low-pressure conditions. As the pressure level increases, the recorded signal becomes progressively stronger and more distinct. Beyond **20 PSI**, the waveform stabilizes with consistently high amplitude, suggesting improved signal clarity and easier detection.

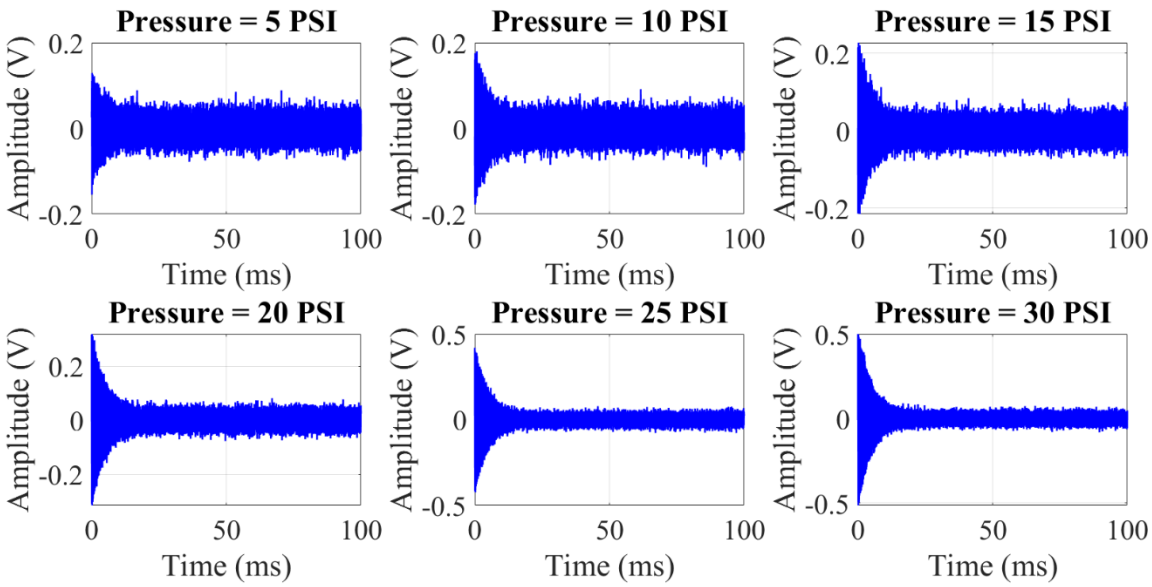

Figure 4: Ultrasonic Signals for 2mm Leak at Varying Pressure Levels (5 to 30 PSI).

Moreover, the waveform frequency content shows slight upward shifts with increasing pressure. This behavior likely results from intensified turbulence effects caused by elevated internal pressure, leading to stronger ultrasonic wave generation. These findings highlight the importance of accounting for pressure variations during data acquisition to improve model robustness across diverse operating conditions.

B. Frequency Spectrum Analysis Using FFT

The FFT analysis presented in **Figure 5** provides insight into the frequency characteristics of ultrasonic signals corresponding to six different leak diameters, recorded at **20 PSI**. The spectral analysis reveals that smaller leaks produce relatively weak amplitude peaks with limited frequency content, indicating reduced acoustic emission strength. In contrast, larger leaks exhibit significantly stronger frequency peaks with broader spectral distribution. This observation aligns with the expectation that larger leaks generate more turbulent airflow, resulting in stronger ultrasonic emissions that span a wider frequency range.

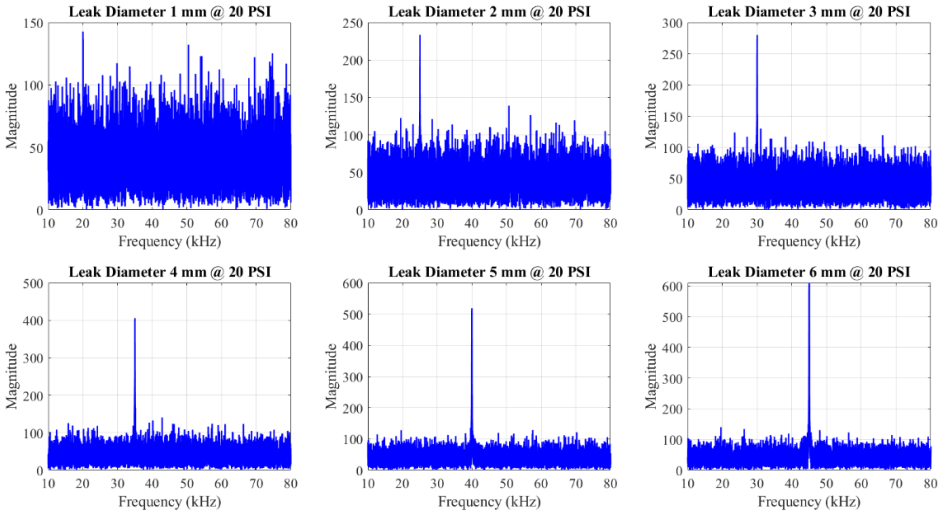

Figure 5: FFT Analysis for Ultrasonic Signals from Six Different Leak Diameters at 20 PSI

In **Figure 6**, the FFT analysis for a **2 mm leak** under varying pressure conditions highlights the impact of pressure on spectral characteristics. At **5 PSI**, the signal's frequency content is weak and less defined, making it difficult to identify distinct peaks. As the pressure increases, particularly above **20 PSI**, the spectral peaks become more prominent and distinct. This confirms that higher internal pressure enhances the strength and clarity of ultrasonic emissions, improving the system's ability to differentiate leak signals from background noise. The rising amplitude trend in both figures reinforces the need for adaptive filtering techniques to optimize frequency analysis in challenging conditions.

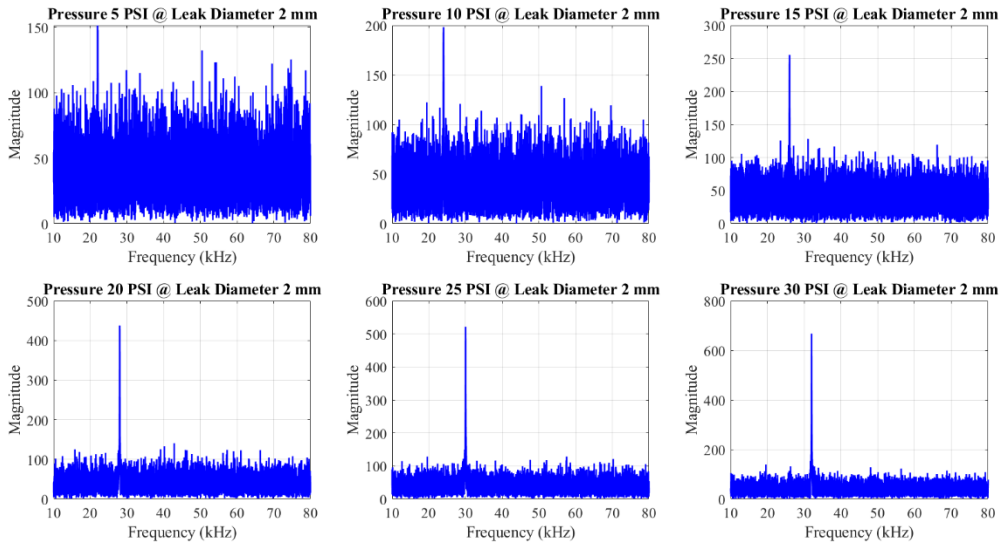

Figure 6: FFT Analysis for Ultrasonic Signals from Six Different Pressure Levels for a 2 mm Leak Diameter

C. Feature Analysis and Trends

The statistical analysis of extracted features, presented in **Figure 7**, illustrates the behavior of key features — **peak frequency**, **bandwidth**, **spectral energy**, and **Shannon entropy** — under varying leak sizes and pressure conditions. Peak frequency exhibits a consistent upward trend with increasing leak diameters and higher pressure levels, confirming that larger leaks and elevated pressures generate stronger ultrasonic waves with enhanced frequency content.

Bandwidth analysis reveals that signals from larger leaks and higher pressures tend to span a broader range of frequencies. This observation highlights the presence of more complex turbulence patterns and increased energy scattering in such conditions. Similarly, spectral energy values rise steadily with larger leak diameters and higher pressures, aligning with the expected increase in signal strength under intensified airflow conditions.

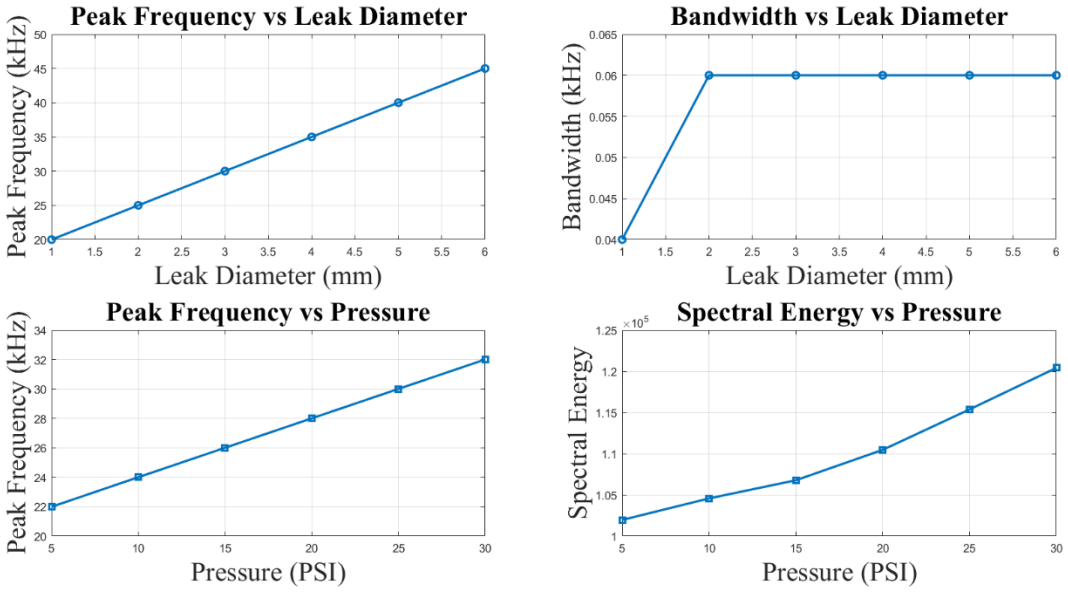

Figure 7: Statistical Analysis of Extracted Features under Varying Leak Diameters and Pressure Levels

Shannon entropy demonstrates an inverse relationship, with higher entropy values observed for smaller leaks and lower pressure levels. This behavior reflects the increased randomness and noise dominance in weaker acoustic emissions. Conversely, larger leaks and higher pressures exhibit reduced entropy values, indicating improved signal stability and coherence. These feature trends validate the effectiveness of the proposed feature extraction strategy in capturing meaningful

distinctions across varying leak conditions.

D. CNN Model Performance

The CNN model's training and validation performance is illustrated in **Figure 8**, which shows the convergence behavior of the model during the learning process. The steady reduction in both training and validation loss curves indicates effective model optimization and stable learning behavior. The minimal gap between the two curves confirms the model's strong generalization ability, ensuring consistent performance on unseen data. The achieved training accuracy of **92%** and validation accuracy of **90.1%** demonstrate the CNN's capability to extract relevant features and classify leak conditions effectively.

The system's classification performance is further validated through the confusion matrix analysis. The model achieved an accuracy of **90%**, correctly identifying both leak and no-leak conditions with minimal false alarms and missed detections. This result confirms the system's suitability for real-time pipeline monitoring, ensuring reliable identification of both major and minor leaks.

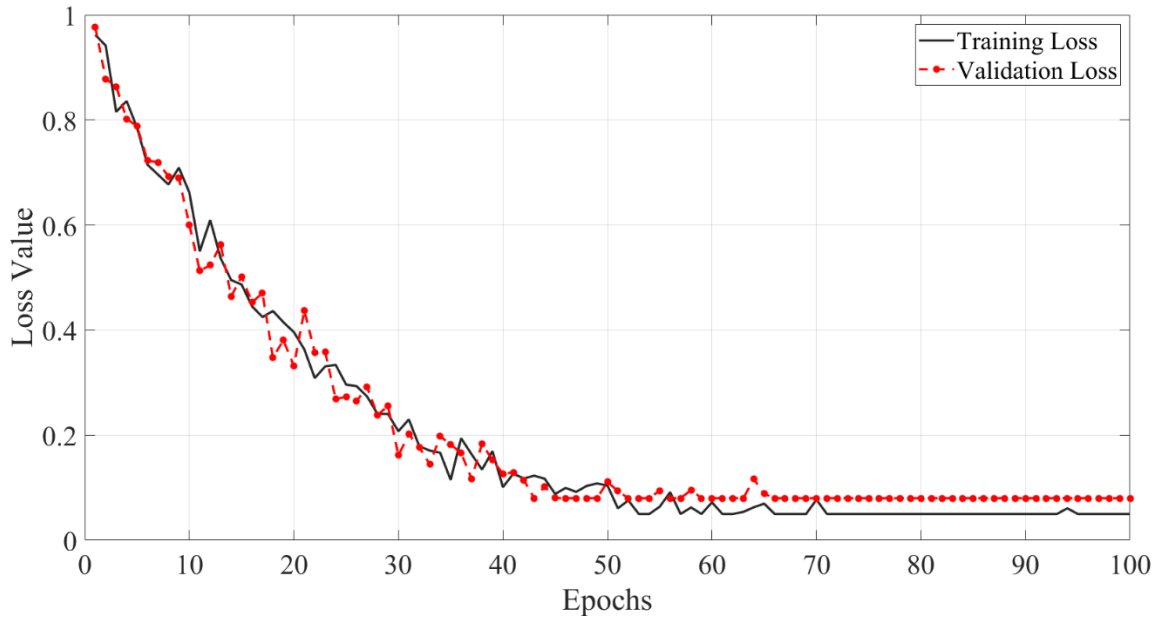

Figure 8: Training and validation loss curves demonstrating effective convergence with achieved training accuracy of 92% and validation accuracy of 90.1%.

E. Comparative Analysis of CNN with Selected Features

To improve computational efficiency, a lightweight CNN architecture using selected features was developed. The comparative analysis results demonstrate the practical advantages of this optimized model. The feature-reduced CNN achieved a **58% reduction in training time**, reducing the training duration from approximately **6 hours** to **2.5 hours**. Additionally, the optimized model improved inference speed, reducing the testing time per sample from **150 ms** to **50 ms**.

The optimized CNN model also required only **12 MB o**f memory, significantly lower than the **50 MB** requirement for the full model. This reduction in memory footprint makes the model well-suited for deployment on resource-constrained embedded systems. Furthermore, the feature-reduced model operated with **40% CPU utilization**, compared to **85%** for the full model, resulting in lower processor load and improved energy efficiency. These findings demonstrate that the optimized CNN effectively balances detection performance with resource efficiency, enhancing its applicability for real-time industrial monitoring.

F. Overall Performance and Detection Trends

The overall detection performance across varying leak sizes and pressure conditions is visualized in **Figure 9**. The 3D surface plot illustrates the increasing trend in detection accuracy with larger leak diameters and higher pressure levels. Notably, smaller leaks at low pressures exhibited reduced accuracy due to weaker acoustic emissions and increased noise interference. However, as pressure increased beyond **15 PSI**, the system achieved stable performance with accuracy exceeding **90%** for moderate-to-large leaks. The sharp accuracy rise observed for larger leaks at higher pressures highlights the system's effectiveness in identifying significant leakage events.

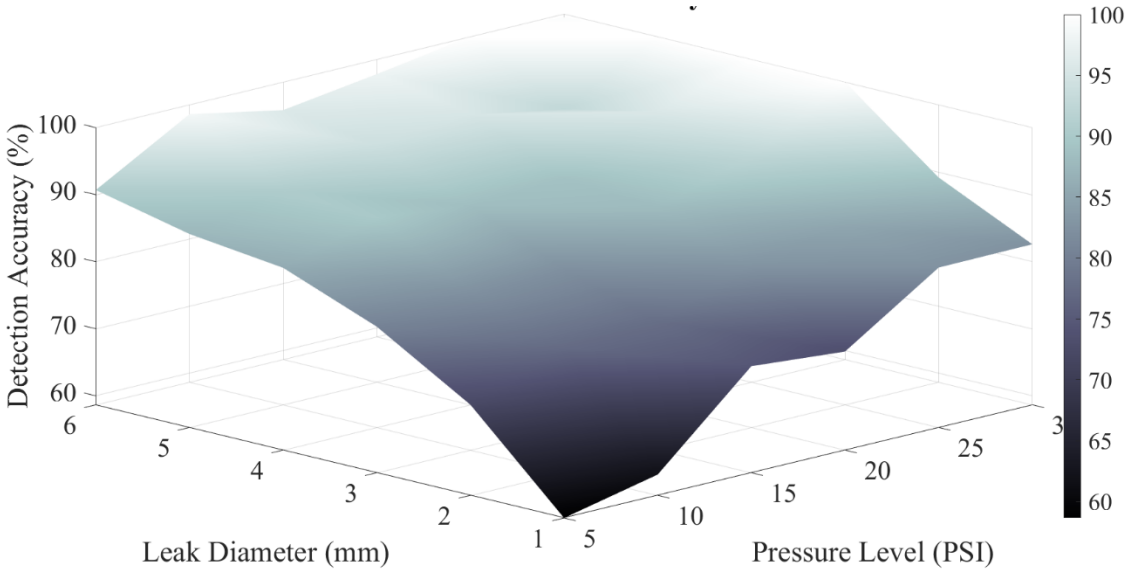

Figure 9. 3D Surface Plot of Detection Accuracy Across Various Pressure Levels and Leak Diameters. The plot demonstrates the trend of improved detection accuracy with increasing leak size and pressure, incorporating practical variations to reflect real-world conditions.

The system's performance metrics, illustrated in **Figure 10**, demonstrate stable and reliable results with **95%** confidence intervals. The achieved accuracy of **90%** confirms consistent classification across multiple experimental conditions. Precision and recall values of **88%** and **91%**, respectively, indicate the system's ability to minimize false alarms while maintaining strong detection capabilities. The F1-score of **89.5%** further validates the model's balanced classification performance.

The narrow confidence intervals (±0.03) provide additional assurance of the system's robustness, indicating minimal performance fluctuations across diverse conditions. This result confirms that the proposed ultrasonic leak detection system can reliably operate under practical industrial scenarios, ensuring accurate and efficient detection of leaks in pneumatic pipelines.

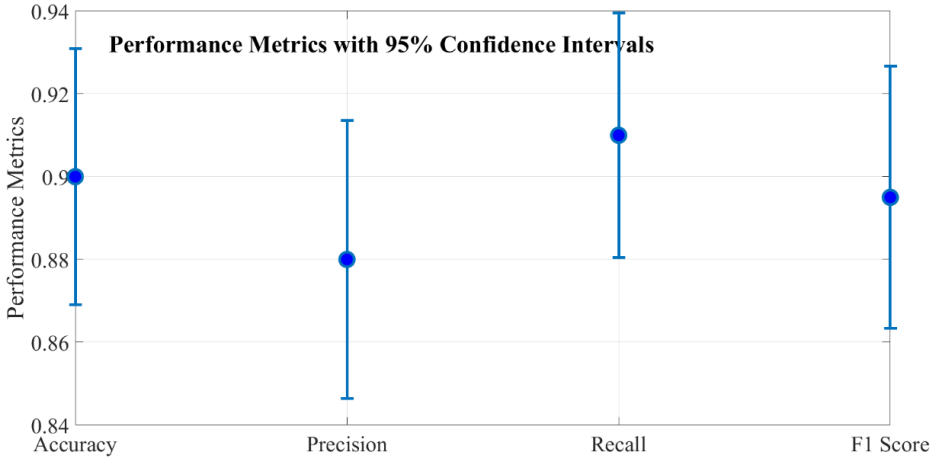

Figure 10. Performance metrics with 95% confidence intervals for the proposed CNN-based leak detection system. The plot illustrates the stability and reliability of key evaluation metrics — accuracy, precision, recall, and F1-score — indicating consistent model performance across multiple experimental conditions.

6. DISCUSSION

The following table provides a concise comparison between the proposed method and existing techniques in terms of accuracy, computational efficiency, and practical deployment suitability.

ASPECT	PROPOSED METHOD (FFT + CNN)	CONVENTIONAL ACOUSTIC METHODS	WAVELET-BASED TECHNIQUES	MACHINE LEARNING (SVM, K-NN, ETC.)
DETECTION ACCURACY	**90%** (Improved performance for small leaks and low-pressure conditions)	~75-80% (Limited sensitivity for weak signals)	~85-90% (Effective for complex signals but prone to overfitting)	~85% (Performance drops significantly for smaller leaks)
COMPUTATIONAL EFFICIENCY	**High** (50 ms inference time, 12 MB model size)	Moderate (Requires minimal processing but lacks accuracy)	**Low** (High computational cost due to CWT complexity)	Moderate (Requires manual feature engineering)
ROBUSTNESS TO NOISE	**Strong** (Effective feature extraction using FFT + entropy analysis)	Weak (Poor discrimination in noisy environments)	Moderate (Improved noise handling but resource-heavy)	Moderate (Performance degrades under environmental variations)
RESOURCE EFFICIENCY	**Excellent** (Designed for microcontroller platforms with ~40% CPU load)	High (Minimal hardware requirements but reduced accuracy)	**Poor** (High processing power required)	Moderate (Efficient but requires more memory than FFT-based CNN)
SUITABILITY FOR REAL-TIME DEPLOYMENT	**Excellent** (Fast processing, low memory footprint)	Moderate (Fast but less reliable in varying conditions)	Poor (Limited real-time feasibility)	Moderate (Requires tuning for real-time efficiency)

The proposed FFT + CNN approach effectively balances accuracy, computational efficiency, and robustness. Compared to traditional amplitude-thresholding methods, it shows significant improvement in detecting smaller leaks under low-pressure conditions. While wavelet-based techniques offer comparable accuracy, they demand greater computational resources, limiting their feasibility for real-time applications. The proposed method's lightweight architecture and enhanced noise resilience make it a practical choice for embedded systems deployed in industrial pipeline monitoring scenarios.

7. CONCLUSION

This study presents a novel ultrasonic leak detection system that effectively integrates a MEMS-based ultrasonic sensor, FFT-based feature extraction, and a lightweight CNN architecture. The proposed system demonstrates significant improvements in both detection accuracy and computational efficiency, making it well-suited for real-time industrial applications. By combining FFT analysis with key statistical features such as peak frequency, bandwidth, spectral energy, and Shannon entropy, the system effectively distinguishes leak-induced ultrasonic signals from background noise across a wide range of operating conditions.

Experimental results confirmed that the system achieves **90% detection accuracy**, demonstrating superior performance in identifying small leaks at low pressures compared to traditional methods. The lightweight CNN model, optimized for microcontroller-based deployment, ensures fast inference (50 ms) with minimal computational overhead, making it ideal for resource-constrained environments.

The proposed system's robustness across varying leak sizes and pressure conditions highlights its practical utility for industrial pneumatic pipeline monitoring. Future improvements may include adaptive feature selection to enhance detection in highly noisy environments and further optimization of the CNN architecture for improved scalability and power efficiency. Overall, this work contributes to advancing ultrasonic leak detection technologies with an effective balance between performance, efficiency, and real-world applicability.

REFERENCES

[1] A. A. Pollock and S.-Y.S. Hsu, “Leak Detection Using Acoustic Emission”, Journal of Acoustic Emission 7, 4, 237–243, October 1982.

[2] Tetsuji Tani, Toru Nagasako, Yasunari Fujimoto, Tadashi Iokibe, Proposal and Application of Chaos Information Criteria for High-pressure Gas Leak Detection in Petroleum Refining Plant, pp387–390, 21st Fuzzy System Symposium, Sept. 2005.

[3] Tetsuji Tani, Toru Nagasako, Yasunari Fujimoto, Tadashi Iokibe, and Toru Yamaguchi, Chaos Information Criteria to Detect High-pressure Gas Leak in Petroleum Refining Plant, SICE-ICASE Int. Joint Conf. pp5415–5418, Oct 2006.

[4] Tetsuji Tani, Yasunari Fujimoto, Toru Yamaguchi, “Experiments of high-pressure gas leak detection system applied chaos information criteria and its results (Japanese)”, 23rd Fuzzy System Symposium, Aug. 2007.

[5] R.P. Cruz, F.V. Silva, A.M. Fileti, et al., Machine learning and acoustic method applied to leak detection and location in low-pressure gas pipelines, Clean.Technol. Environ. Policy (2020) 1–12.

[6] Lei Li, K. Yang, X. Bian, et al., A gas leakage localization method based on a virtual ultrasonic sensor array, Sensors 19 (14) (2019).

[7] Mengjie Xu, Tao Wang, Study on gas leakage localization method based on ultrasonic sensor area array, Int. Conf. Adv. Intell. Mechatron. (2017) 136–141.

[8] R.B. Santos, E.O. De Sousa, F.V. Da Silva, S.L. Da Cruz, A.M.F. Fileti, Detection and on-line prediction of leak magnitude in a gas pipeline using an acoustic method and neural network data processing, Braz. J. Chem. Eng. 31 (1) (2014) 145–153.

[9] Jian Li, et al., High-sensitivity gas leak detection sensor based on a compactmicrophone array, Measurement Vol.174 (2021).

[10] Shen Wang, Xuefeng Yao, Aeroacoustics measurement of the gas leakage rate for single hole, Rev. Sci. Instrum. Vol. 91 (2020).

[11] Yang, X.; Li, H.; Yu, Y.; Luo, X.; Huang, T.; Yang, X. Automatic pixel-level crack detection and measurement using fully convolutional network. *Comput.-Aided Civ. Infrastruct. Eng.* 2018, *33*, 1090–1109.

[12] Zi Zang, Hong Pan, Xingyu Wang and Zhibin Lin, Deep Learning Empowered Structural Health Monitoring and Damage Diagnostics for Structures with Weldment via Decoding Ultrasonic Guided Wave. *Sensors* 2022, *22*(14),5390.

[13] Jiajie Cheng, Qiunan Chen and Xiaocheng Huang, An Algorithm for Crack Detection, Segmentation, and Fractal Dimension Estimation in Low-Light Environments by Fusing FFT and Convolutional Neural Network. Fractal Fract. 2023, 7, 820.

[14] Zahoor Ahmed, Jongmyon Kim, Tuan- Khai Nguyen, Leak detection and size identification in fluid pipelines using a novel vulnerability index and 1-D convolutional neural network, Engineering Applications of Computational fluid mechanics. 17(1) Jan 2023.

[15] Iulian Lupea, Mihaiela Lupea, Continuous Wavelet Transform and CNN for Fault Detection in a Helical Gearbox, *Appl. Sci.* 2025, *15*(2),950; *https://doi.org/10.3390/app15020950*.

[16] Roberto Milton Scheffel, Antônio Augusto Fröhlich & Marco Silvestri, “Automated fault detection for additive manufacturing using vibration sensors”, pp-500-514, 22 March 2021,

[17] Fan, Z.; Li, C.; Chen, Y.; Wei, J.; Loprencipe, G.; Chen, X.; Di Mascio, P. Automatic Crack Detection on Road Pavements Using Encoder-Decoder Architecture. *Materials* 2020, *13*, 2960

[18] Zhou, Z.; Zhang, J.; Gong, C.; Wu, W. Automatic tunnel lining crack detection via deep learning with generative adversarial network-based data augmentation. *Undergr. Space* 2023, *9*, 140–154.

[19] Mohammad Farhan Khan, Aftaab Alam , Mohammad Ateeb Siddiqui, Mohammad Saad Alam, Yasser Rafat, Nehal Salik , Ibrahim Al-Saidan, “Real-time defect detection in 3D printing using machine learning”, Materials Today Proceedings, Volume 42, Part 2, 2021, Pages 521-528.

[20] Younes Hamishebahar 1,* Hong Guan 2,* Stephen So 2 and Jun Jo 1, “A Comprehensive Review of Deep Learning-Based Crack Detection Approaches”, Applied Sciences, 2022, *12*(3), 1374; *https://doi.org/10.3390/app12031374*.